



Wu Tangzhen · Yu Xun · Wu Zhen · Zhao Donglin ·
Ren Xiaohui

A novel finite element formulation based on five unknown model for free vibration analysis of circular and ellipse sandwich plates

Received: 21 June 2022 / Accepted: 4 December 2022 / Published online: 17 December 2022
© The Author(s), under exclusive licence to Springer-Verlag GmbH Germany, part of Springer Nature 2022

Abstract To investigate the dynamic response of circular and ellipse sandwich plates, a higher-order model with five displacement parameters has been proposed, which can fulfill compatible conditions of transverse shear stresses at the interfaces. Based on the proposed model, the finite element formulation has been developed, where the refined-element method is utilized to solve the compatible relation of first derivatives of transverse displacement on the common edges of adjacent elements. By analyzing free vibration of sandwich plates made up of aluminum/composite face sheets and polymethacrylimide core, the performance of the proposed model has been verified. In addition, influence of material properties and geometric parameters on natural frequencies has been also investigated. Results show that displacement modes in the ellipse plate differ from those of the circular plate attributing to different stiffness along x and y directions. Moreover, the ratios of major axis to minor axis have a severe impact on natural frequencies of ellipse sandwich plates. Stiffness of sandwich plates can be explicitly improved by applying the composite face sheets. Furthermore, the relative stiffness of sandwich circular plate can be further improved by changing the lamination configuration, which can demonstrate good designability of sandwich plates with composite face sheets.

Keywords Five unknown model · Circular and ellipse plate · Natural frequency

1 Introduction

By assembling the stiff face sheets and the low-density core layer, a light-weight sandwich structure can be designed for the weight-sensitive engineering field, such as aerospace, ships and civil engineering. Structural weight can be reduced efficiently by selecting the well-matched face sheets and the core layer. Nevertheless, analysis of mechanical behaviors in such structures will confront a rigorous challenge, as the large transverse shear deformations have to be deliberated attributing to the sudden change of transverse shear modulus at the interlayer between the face sheet and the core layer. As a result, the classical plate theory (CPT) [1] discarding transverse shear deformation is no longer adaptable to analysis of the mechanical behaviors of sandwich structures. Therefore, numerous investigators have paid more attention to the models deliberating transverse shear deformation.

W. Tangzhen · Y. Xun
China Helicopter Research and Development Institute, Jingdezhen 333001, China

W. Zhen (✉)
School of Aeronautics, Northwestern Polytechnical University, Xi'an 710072, China
e-mail: wuzhenhk@nwpu.edu.cn

Z. Donglin
School of Materials Science and Engineering, Northwestern Polytechnical University, Xi'an 710072, China

R. Xiaohui
School of Mechanical Engineering, Xi'an Aeronautical University, Xi'an 710065, China

In the early stage of exploration on the shear deformation theory, Reissner [2] attempted to research the impact of transverse shear deformation on static response of plates. Mindlin [3] assumed transverse shear deformation to be linear distribution along the thickness of plate, so that the first-order shear deformation theory (FSDT) can be established by utilizing such assumption. The FSDT has been utilized to deliberate mechanical behaviors of isotropic, functionally graded material (FGM) and orthotropic plates attributing to its flexibility and efficiency. For the sandwich plates with low-density core, transverse shear deformation will suddenly change at the adjacent laminates attributing to large diversion of transverse shear moduli between the face sheets and the core. Evidently, the FSDT is not adaptable to simulation of such large transverse shear deformation, so that the correction factor has to be selected to elevate prediction of transverse shear deformation. Nonetheless, reasonable selection of the correction factors severely depends on material characteristics. For the sake of conquering limitation of the FSDT, the inspiration deriving from three-dimensional (3D) elasticity theory [4, 5] inspired investigators to establish the higher-order shear deformation theory (HSDT).

Whitney and Sun [6] attempted to establish a HSDT for analysis of layered plates. Reddy [7] developed a delicate higher-order theory with five independent unknowns, which can simulate the parabolic distributions of transverse shear deformation across thickness of plate. Furthermore, the free condition of transverse shear stresses on surfaces can be met in advance. Reddy's model can yield the more precise results contracted to those acquired from the FSDT. Advantages of HSDT contrasting to FSDT motivate researchers to construct various HSDTs [8, 9]. Meiche et al. [10] established a hyperbolic-type HSDT with four unknowns to calculate natural frequencies and buckling loads of FGM sandwich plates subjected to four simply-supported edges. Matsunaga [11–13] established a series of HSDTs to explore an impact of higher-order shear deformation on dynamic and buckling behaviors of layered and sandwich plates. In the light of Reddy's HSDT [7], Nayak et al. [14] constructed a plate element to produce natural frequencies of layered and sandwich plates. Taking advantage of Reddy's HSDT, Jin et al. [15] deliberated influence of boundary conditions on dynamic response of sandwich structures. What's more, Tomar and Talha [16] made use of Reddy's HSDT to research the bending and vibration problems of the FGM sandwich plates by deliberating the influence of material uncertainties. Bennoun et al. [17] established a five-unknown theory to deal with free vibration problems of FGM sandwich plates. However, the existing investigations [18, 19] indicated that the HSDTs neglecting continuity conditions of transverse shear stresses at the interfaces will encounter difficulty to produce accurately natural frequencies of the sandwich plate made up of soft core.

What's more, layerwise theories in conjunction with finite element method have been established to yield accurate results [20]. Even so, the displacement variables in layerwise model augment with increase of layer number, so that tedious and complex calculation is to be needed. According to three-dimensional elasticity [4], in-plane displacements are required to be the zig-zag distribution through the thickness direction. By drawing a linear zig-zag function in the in-plane displacement of FSDT, Murakami [21] established a zig-zag model to describe the zig-zag distribution of in-plane displacements. However, such zig-zag model [21] will meet trouble to produce precisely transverse shear stresses directly from constitutive relation. Accurate transverse shear stresses impact largely prediction of natural frequencies of sandwich plates [22]. Based on Kirchhoff–Love plate theory, Orakdögen et al. [23] constructed two quadrilateral elements to study the coupling effect of extension and bending for the functionally graded plates. Making use of the first-order shell theory and Donnell kinematics assumption, Sofiyev and Osmancebioglu [24] investigated carefully influence of functionally graded coatings on dynamic behaviors of sandwich-truncated conical shells, and some valuable conclusions have been drawn. Subsequently, buckling behaviors of sandwich-truncated conical shells composed of functionally graded materials have been investigated in detail by Sofiyev [25] via utilizing the first-order theory. Hacıyev et al. [26] researched the vibration behaviors of functionally graded (FG) rectangular plates resting on elastic foundations, where effects of material parameters including material gradient and orthotropy on dynamic response have been analyzed in detail. In order to propose the methodological solutions of the pure FG structures and the FG sandwich constructions, Sofiyev [27] presented an exhaustive review on the published theories and models for the FG conical shells, FG-layered conical shells and the FG sandwich conical shells, which can provide a valuable reference for other investigators. Recently, based on the shear deformation theory, Sofiyev and Fantuzzi [28] proposed a novel approach to investigate vibration and stability behaviors of clamped sandwich cylindrical shells with the FG coatings.

By means of the hyperbolic shear deformation model, Avcar et al. [29] analyzed dynamic response of sigmoid FG sandwich beams, and influence of layup schemes of the FG sandwich beams on natural frequencies has been explored in detail. Hadji and Avcar [30] further utilized the hyperbolic shear displacement theory to study influence of boundary conditions, porosity volume fraction and layup scheme on free vibration of the FG sandwich plates. Based on the layerwise model, Belarbi et al. [31] constructed a new element to analyze free

vibration of multilayered sandwich plates, and the good performance of the proposed model has been verified by several examples. On the basis of the third-order model, Hadji et al. [32] investigated dynamic behaviors of the imperfect FG sandwich plates resting on elastic foundation, and the instructive conclusions have been presented. In addition, Hirane et al. [33] proposed a novel higher-order finite element model to investigate static and dynamic behaviors of FG sandwich plates. Based on the higher-order zig-zag model, Garg et al. [34] constructed a finite element formulation to study vibration and buckling response of the FG sandwich plates. In terms of a new hyperbolic theory, Vinh and Huy [35] proposed a four-node quadrilateral element to research the bending, buckling and dynamic behaviors of the FG plates. Moreover, impact of porosity distribution on mechanical response of FG sandwich plates has been evaluated carefully. Making use of the improved first-order theory and the mixed finite element formulation, Vinh et al. [36] developed a four-node plate element to study the buckling and the bending behaviors of bi-directional FG plates, and some remarkable conclusions have been presented. In addition, the advancement of theory, new design and application trend for sandwich structures are summarized by Birman and Kardomateas [37].

As it is clear, most researches by means of the different models have been limited to rectangular plates. In fact, the mechanical characteristics of circular and elliptic plates utilized in repairment are extremely important as well. Ebrahimi and Rastgo [38] explored the free vibration behaviors of FGM piezoelectric sandwich circular plate by utilizing analytical method relying on the CPT. In the light of the FSDT, a mathematical derivation of free flexural vibration for the three-layer piezoelectric circular plate was made by Liu et al. [39]. Qiu et al. [40] established an analytical model to research dynamic behaviors of circular sandwich plates under shocking loads. Du and Ma [41] attempted to study impact of diverse loads on the nonlinear vibration characteristics of sandwich circular plates. In the light of the Reddy's HSDT [7], Hashemi et al. [42] explored the dynamic behaviors of the piezoelectric FGM annular plates with diverse thickness-radius ratios and boundary conditions. What's more, Sharma and Parashar [43] and Jandaghian et al. [44] also made an exhaustive analysis on the dynamic behaviors of FGM piezoelectric circular plates. Furthermore, vibration regulation of circular piezolaminated and sandwich plates was investigated relying on the nonfragile control strategy [45]. For the vibration of annular sandwich plates, other researchers have also carried out a series of studies which can be seen in literature [46, 47]. Recently, Shishehsaz et al. [48] predicted stress distribution in the circular plate by means of layerwise theory and the hyperbolic HSDT. Shahrokhi et al. [49] attempted to investigate effect of length scale and electric field on the vibrational behaviors of circular sandwich micro-plates.

Survey of literature shows that numerous theories and the finite element methods have been established for the analysis of rectangular sandwich plates and shells. However, investigations on dynamic characteristic of the circular and ellipse sandwich structures made up of aluminum/composite face sheets and PMI core are less reported. In order to accurately predict dynamic response of the circular and ellipse sandwich structures, a higher-order model with five independent unknowns will be established. The proposed model can fulfill in advance continuity conditions of transverse shear stresses at the interfaces between adjacent layers, which can improve accuracy in predicting natural frequencies. For the free vibration of sandwich circular and ellipse plates with clamped boundaries, it is hard to present an analytical solution. In the light of the present model, a three-node triangular element in conjunction with the refined-element method [50] is to be developed for dynamic analysis of sandwich circular and ellipse plates. For the sake of appraising capability of the five-unknown higher-order models for free vibration of circular and ellipse sandwich plates, the present work tries to implement three types of five-unknown higher-order models proposed by Shi et al. [51], Kumar et al. [52] and Shukla et al. [53] by utilizing the same finite element method. In addition, results acquired from the three-dimensional finite element method (3D-FEM) are also selected as the reference solutions to appraise the present model as well as other models. This work establishes an alternative method to elevate the capability yielding accurately natural frequencies of sandwich circular and ellipse plates without augment of any additional displacement variables.

2 A novel finite element formulation (RFEF)

2.1 A higher-order model with five independent variables

It is well known that Reddy's model [7] has been widely utilized for mechanical analysis of composite and sandwich plates attributing to its efficiency and accuracy. In the Reddy's model, rotation of the normal is divided into the transverse shear components and the derivatives of deflection with respect to x and y , so that it is convenient to construct reasonably transverse shear components for accurate analysis of composite

plates with hybridized laminates. In the light of such assumption, a Reddy-type higher-order model with five unknowns is to be presented in present work. Compared to the classical Reddy's model, the compatible conditions of transverse shear stresses at the adjacent laminates will be enforced in advance.

To acquire the improved Reddy's model, the classical Reddy's model should be recalled, which can be presented by

$$\begin{aligned} u(x, y, z) &= u_0(x, y) + f(z)\gamma_x(x, y) - zw_x(x, y) \\ v(x, y, z) &= v_0(x, y) + f(z)\gamma_y(x, y) - zw_y(x, y) \\ w(x, y, z) &= w_0(x, y) \end{aligned} \quad (1)$$

in which u_0 , v_0 and w_0 represent the displacements on the mid-plane of plate along x and y directions; γ_x and γ_y signify the transverse shear components; w_x and w_y denote separately the derivatives of deflection with respect to y and x axes.

According to three-dimensional elasticity theory [4], transverse shear stress components should be compatible at the interfaces of adjacent laminates. For a sandwich plate with form core, transverse shear modulus suddenly changes at common surface of adjacent laminates, which will induce a large transverse shear deformation. Thereby, it is required to construct a transverse shear deformation function $f(z)$ with a good performance. To achieve this goal, local displacement functions will be utilized at each laminate. By inserting the second-order local functions into displacement field, the displacements at arbitrary point of plate can be described as

$$\begin{aligned} u(x, y, z) &= u_0(x, y) + f(z)\gamma_x(x, y) - zw_x(x, y) + \varsigma_k u_1^k(x, y) + \varsigma_k^2 u_2^k(x, y) \\ v(x, y, z) &= v_0(x, y) + f(z)\gamma_y(x, y) - zw_y(x, y) + \varsigma_k v_1^k(x, y) + \varsigma_k^2 v_2^k(x, y) \\ w(x, y, z) &= w_0(x, y) \end{aligned} \quad (2)$$

where transverse shear function developed by Reddy [7] $f(z) = z(1 - 4z^2/3h^2)$, in which h denotes whole thickness of plate; ς_k signifies the thickness coordinate at the k th laminate. Relationship between the local coordinate ς_k and the global coordinate z can be expressed as

$$\varsigma_k = c_1^k z - c_2^k \quad (3)$$

in which $c_1^k = 2/(z_{k+1} - z_k)$, $c_2^k = (z_{k+1} + z_k)/(z_{k+1} - z_k)$, where z_{k+1} signifies the thickness coordinate at the interface between the k th layer and $(k + 1)$ th layer.

In Eq. (2), it is found that four displacement parameters u_1^k , u_2^k , v_1^k and v_2^k are involved in the k th laminate. For a composite plate made up of N laminates, $4N$ additional displacement variables will be introduced. In order to decrease calculational cost, these additional variables should be reduced without compromising accuracy. As a result, making use of compatible conditions of displacements at the common interfaces between adjacent laminates, the variables at each laminate can be reduced, which can be expressed as

$$\begin{aligned} u_2^k(x, y) &= u_1^k(x, y) + u_1^{k-1}(x, y) + u_2^{k-1}(x, y) \\ v_2^k(x, y) &= v_1^k(x, y) + v_1^{k-1}(x, y) + v_2^{k-1}(x, y) \end{aligned} \quad (4)$$

where k is always more than one.

To further reduce displacement parameters, the compatible conditions of transverse shear stresses between the k th laminate and $(k-1)$ th laminate will be enforced, which may be given by

$$\begin{aligned} \tau_{xz}^k(x, y, z_k) &= \tau_{xz}^{k-1}(x, y, z_k) \\ \tau_{yz}^k(x, y, z_k) &= \tau_{yz}^{k-1}(x, y, z_k) \end{aligned} \quad (5)$$

For free vibration problems, the lower and upper surfaces of sandwich plates do not subject to any loadings. Therefore, transverse shear stresses on the lower and upper surfaces should be equal to be zero, so the following equation can be given by

$$\begin{aligned} \tau_{xz}^1(x, y, z_1) &= \tau_{xz}^N(x, y, z_{N+1}) = 0 \\ \tau_{yz}^1(x, y, z_1) &= \tau_{yz}^N(x, y, z_{N+1}) = 0 \end{aligned} \quad (6)$$

where N denotes the total number of layers.

Once the constrained conditions above mentioned are fulfilled, all displacement parameters depending on laminates can be completely removed from the initial displacement field. As a result, the proposed Reddy-type higher-order model can be presented by

$$\begin{aligned}
 u(x, y, z) &= u_0(x, y) + f_u^k(z)\gamma_x(x, y) - zw_x(x, y) \\
 v(x, y, z) &= v_0(x, y) + f_v^k(z)\gamma_y(x, y) - zw_y(x, y) \\
 w(x, y, z) &= w_0(x, y)
 \end{aligned}
 \tag{7}$$

In Eq. (7), it can be found that the form of the present model is nearly the same as that of Reddy’s model [7], and transverse shear functions through thickness direction $f_u^k(z)$ and $f_v^k(z)$ only differ from those of Reddy’s model. Furthermore, the proposed model can meet compatible conditions of transverse shear stresses at the interfaces, which can elevate accuracy predicting natural frequencies of sandwich plates. In addition, the zig-zag effect of in-plane displacements has been also taken into account in the proposed model, which is induced by the mismatching material properties at the adjacent layers.

Transverse shear functions $f_u^k(z)$ and $f_v^k(z)$ can be determined by utilizing the constrained conditions of displacements and stresses, which can be explicitly shown as follows

$$\begin{aligned}
 f_u^k(z) &= \lambda_1^k \zeta_k + \lambda_2^k \zeta_k^2 + f(z) \\
 f_v^k(z) &= \kappa_1^k \zeta_k + \kappa_2^k \zeta_k^2 + f(z)
 \end{aligned}
 \tag{8}$$

where $f(z)$ is the transverse shear function proposed by Reddy [7].

$$\begin{aligned}
 \lambda_i^k &= F_{i1}^k L + F_{i2}^k \\
 \kappa_i^k &= H_{i1}^k M + H_{i2}^k
 \end{aligned}
 \tag{9}$$

where coefficients $F_{i1}^k, F_{i2}^k, H_{i1}^k$ and H_{i2}^k can be determined by using the compatible conditions of transverse shear stresses.

In the light of the compatible conditions of transverse shear stresses at the interfaces, the following equations can be presented by

$$\begin{aligned}
 F_{11}^k &= -(2 + \alpha_1^k)F_{11}^{k-1} - 2(1 + \alpha_1^k)F_{21}^{k-1} \\
 F_{12}^k &= -(2 + \alpha_1^k)F_{12}^{k-1} - 2(1 + \alpha_1^k)F_{22}^{k-1} + \alpha_2^k \\
 F_{21}^k &= F_{11}^k + F_{11}^{k-1} + F_{21}^{k-1} \\
 F_{22}^k &= F_{12}^k + F_{12}^{k-1} + F_{22}^{k-1} \\
 H_{11}^k &= -(2 + \beta_1^k)H_{11}^{k-1} - 2(1 + \beta_1^k)H_{21}^{k-1} \\
 H_{12}^k &= -(2 + \beta_1^k)H_{12}^{k-1} - 2(1 + \beta_1^k)H_{22}^{k-1} + \beta_2^k \\
 H_{21}^k &= H_{11}^k + H_{11}^{k-1} + H_{21}^{k-1} \\
 H_{22}^k &= H_{12}^k + H_{12}^{k-1} + H_{22}^{k-1}
 \end{aligned}
 \tag{10}$$

whereas $k = 1, F_{11}^k = H_{11}^k = 1, F_{12}^k = H_{12}^k = 0; F_{21}^k = H_{21}^k = 1/2, F_{22}^k = H_{22}^k = (1 - 4z_k^2/h^2)/(2c_1^k)$; as k is more than one, F_{ij}^k and H_{ij}^k can be obtained by Eq. (10).

$$\begin{aligned}
 \alpha_1^k &= (c_1^{k-1} Q_{44}^{k-1}) / (c_1^k Q_{44}^k) \\
 \alpha_2^k &= (Q_{44}^k - Q_{44}^{k-1})(1 - 4z_k^2/h^2) / (c_1^k Q_{44}^k) \\
 \beta_1^k &= (c_1^{k-1} Q_{55}^{k-1}) / (c_1^k Q_{55}^k) \\
 \beta_2^k &= (Q_{55}^k - Q_{55}^{k-1})(1 - 4z_k^2/h^2) / (c_1^k Q_{55}^k)
 \end{aligned}
 \tag{11}$$

in which $Q_{44}^k = G_{13}^k$ and $Q_{55}^k = G_{23}^k$, where G_{13}^k and G_{23}^k denote the shear moduli in 1–3 plane and 2–3 plane, respectively.

Coefficients L and M can be determined by using the free-surface conditions of transverse shear stresses on the upper surfaces, which are presented by

$$\begin{aligned} L &= -\left(c_1^N F_{12}^N + 2c_1^N F_{22}^N + (1 - 4z_{N+1}^2/h^2)\right) / \left(c_1^N F_{11}^N + 2c_1^N F_{21}^N\right) \\ M &= -\left(c_1^N G_{12}^N + 2c_1^N G_{22}^N + (1 - 4z_{N+1}^2/h^2)\right) / \left(c_1^N G_{11}^N + 2c_1^N G_{21}^N\right) \end{aligned} \tag{12}$$

In order to appraise the proposed model, several Reddy-type higher-order models [51–53] recently reported in the literature will be selected for comparison.

2.2 Finite element formulation based on the proposed model

In present work, free vibration of sandwich circular and ellipse plates with clamped boundaries will be investigated, so that it is hard to present an analytical solution. To extend the proposed model for dynamic analysis of circular and ellipse sandwich plates, the finite element formulation of a three-node triangular element by means of the present model is to be established.

Displacement parameters in the plane can be expressed by using the area coordinates and nodal displacements, so that the displacement parameters u_0, v_0, γ_x and γ_y within one element can be presented by

$$\begin{aligned} u_0 &= \sum_{i=1}^3 L_i u_{0i}, & \gamma_x &= \sum_{i=1}^3 L_i \gamma_{xi} \\ v_0 &= \sum_{i=1}^3 L_i v_{0i}, & \gamma_y &= \sum_{i=1}^3 L_i \gamma_{yi} \end{aligned} \tag{13}$$

where L_i represents the area coordinate, and $i = 1 \sim 3$.

For the present model, the first partial derivatives of transverse displacement are contained in the displacement field, so in-plane strains will contain the second partial derivatives of transverse displacement. As a result, the first partial derivatives of transverse displacement are required to be compatible on the common edges of elements. For the sake of such requirement, the refined-element method proposed by Cheung and Chen [50] will be recalled. According to the refined-element approach, transverse displacement can be discretized as follows

$$w_0 = \sum_{i=1}^3 (N_i^1 w_i + N_{xi}^1 w_{xi} + N_{yi}^1 w_{yi}) \tag{14}$$

Shape functions in Eq. (14) can be explicitly expressed as

$$\mathbf{N}^1 = [\mathbf{N}_1^1 \ \mathbf{N}_2^1 \ \mathbf{N}_3^1] = \mathbf{N}^0 + \mathbf{P}(\mathbf{B}^c - \mathbf{B}^0) \tag{15}$$

where $\mathbf{P} = [0.5x^2 \ 0.5y^2 \ xy]$.

\mathbf{N}^0 denotes the shape function of the element BCIZ [54], which only satisfies the compatible conditions of transverse displacement on the common edge of adjacent elements. Transverse shear strains in the present model merely include the partial first derivatives of transverse displacement, so the shape function of BCIZ will be used to discretize transverse displacement in transverse shear strain, which can be given as

$$\mathbf{N}^0 = [\mathbf{N}_1^0 \ \mathbf{N}_2^0 \ \mathbf{N}_3^0] \tag{16}$$

where

$$\begin{aligned} \mathbf{N}_i^0 &= L_i + L_i^2 L_j + L_i^2 L_k - L_i L_j^2 - L_i L_k^2 \\ \mathbf{N}_{xi}^0 &= c_x^k L_i^2 L_j - c_x^j L_i^2 L_k + 0.5(c_x^k - c_x^j) L_i L_j L_k \\ \mathbf{N}_{yi}^0 &= c_y^j L_i^2 L_k - c_y^k L_i^2 L_j + 0.5(c_y^j - c_y^k) L_i L_j L_k \end{aligned} \tag{17}$$

in which $c_x^i = x_k - x_j$, $c_y^i = y_j - y_k$, where x_j, y_j, x_k and y_k signify, respectively, coordinates at the j th and k th nodes.

In terms of refined-element approach, strain matrix \mathbf{B}^c can be given by

$$\mathbf{B}^c = [\mathbf{B}_1^c \ \mathbf{B}_2^c \ \mathbf{B}_3^c] \tag{18}$$

where

$$\mathbf{B}_1^c = \begin{bmatrix} l_1 m_1 - l_3 m_3 & 0.5(l_1^2 y_{21} + l_3^2 y_{13}) & 0.5(l_1^2 x_{12} + l_3^2 x_{31}) \\ l_3 m_3 - l_1 m_1 & 0.5(m_1^2 y_{21} + m_3^2 y_{13}) & 0.5(m_1^2 x_{12} + m_3^2 x_{31}) \\ m_1^2 - m_3^2 & 0.5(l_1^2 x_{12} + l_3^2 x_{31}) & 0.5(m_1^2 y_{21} + m_3^2 y_{13}) \end{bmatrix} \tag{19}$$

in which l_i and m_i signify the cosines of vector normal to the i th edge; $x_{ij} = x_i - x_j$, $y_{ij} = y_i - y_j$. Further rotating the subscript, matrices \mathbf{B}_2^c and \mathbf{B}_3^c can be acquired.

In addition, the matrix \mathbf{B}^0 can be expressed as follows

$$\mathbf{B}^0 = \frac{1}{A} \iint \bar{\mathbf{B}} dx dy \tag{20}$$

where A signifies the area of one element, and $\bar{\mathbf{B}}$ represents the strain matrix of BCIZ.

By means of relationship between displacements and strains, the strain vector at the k th ply can be presented by

$$\boldsymbol{\varepsilon}^k = \mathbf{B} \mathbf{u}^e \tag{21}$$

in which $\mathbf{B} = [\mathbf{B}_1 \ \mathbf{B}_2 \ \mathbf{B}_3]$, $\mathbf{u}^e = [\mathbf{u}_1 \ \mathbf{u}_2 \ \mathbf{u}_3]^T$, $\mathbf{u}_i = [u_{0i}, v_{0i}, w_{0i}, \gamma_{xi}, w_{xi}, \gamma_{yi}, w_{yi}]$, $i = 1, 2, 3$.

By means of the present model, strain matrix \mathbf{B}_i at the i th node can be written as follows

$$\mathbf{B}_i = \begin{bmatrix} \frac{\partial L_i}{\partial x} & 0 & \mathbf{B}_{1,3} & \Phi_1^k \frac{\partial L_i}{\partial x} & \mathbf{B}_{1,5} & 0 & \mathbf{B}_{1,7} \\ 0 & \frac{\partial L_i}{\partial y} & \mathbf{B}_{2,3} & 0 & \mathbf{B}_{2,5} & \Psi_1^k \frac{\partial L_i}{\partial y} & \mathbf{B}_{2,7} \\ \frac{\partial L_i}{\partial y} & \frac{\partial L_i}{\partial x} & \mathbf{B}_{3,3} & \Phi_1^k \frac{\partial L_i}{\partial y} & \mathbf{B}_{3,5} & \Psi_1^k \frac{\partial L_i}{\partial x} & \mathbf{B}_{3,7} \\ 0 & 0 & \mathbf{B}_{4,3} & \frac{\partial \Phi_1^k}{\partial z} L_i & \mathbf{B}_{4,5} & 0 & \mathbf{B}_{4,7} \\ 0 & 0 & \mathbf{B}_{5,3} & 0 & \mathbf{B}_{5,5} & \frac{\partial \Psi_1^k}{\partial z} L_i & \mathbf{B}_{5,7} \end{bmatrix} \tag{22}$$

where

$$\begin{aligned} \mathbf{B}_{1,3} &= \Phi_2^k \frac{\partial^2 \mathbf{N}_i^1}{\partial x^2}, \mathbf{B}_{1,5} = \Phi_2^k \frac{\partial^2 \mathbf{N}_{xi}^1}{\partial x^2}, \mathbf{B}_{1,7} = \Phi_2^k \frac{\partial^2 \mathbf{N}_{yi}^1}{\partial x^2} \\ \mathbf{B}_{2,3} &= \Psi_2^k \frac{\partial^2 \mathbf{N}_i^1}{\partial y^2}, \mathbf{B}_{2,5} = \Psi_2^k \frac{\partial^2 \mathbf{N}_{yi}^1}{\partial y^2}, \mathbf{B}_{2,7} = \Psi_2^k \frac{\partial^2 \mathbf{N}_{xi}^1}{\partial y^2} \\ \mathbf{B}_{3,3} &= (\Phi_2^k + \Psi_2^k) \frac{\partial^2 \mathbf{N}_i^1}{\partial x \partial y}, \mathbf{B}_{3,5} = (\Phi_2^k + \Psi_2^k) \frac{\partial^2 \mathbf{N}_{xi}^1}{\partial x \partial y}, \mathbf{B}_{3,7} = (\Phi_2^k + \Psi_2^k) \frac{\partial^2 \mathbf{N}_{yi}^1}{\partial x \partial y} \\ \mathbf{B}_{4,3} &= \left(1 + \frac{\partial \Phi_2^k}{\partial z}\right) \frac{\partial \mathbf{N}_i^0}{\partial x}, \mathbf{B}_{4,5} = \left(1 + \frac{\partial \Phi_2^k}{\partial z}\right) \frac{\partial \mathbf{N}_{xi}^0}{\partial x}, \mathbf{B}_{4,7} = \left(1 + \frac{\partial \Phi_2^k}{\partial z}\right) \frac{\partial \mathbf{N}_{yi}^0}{\partial x} \\ \mathbf{B}_{5,3} &= \left(1 + \frac{\partial \Psi_2^k}{\partial z}\right) \frac{\partial \mathbf{N}_i^0}{\partial y}, \mathbf{B}_{5,5} = \left(1 + \frac{\partial \Psi_2^k}{\partial z}\right) \frac{\partial \mathbf{N}_{xi}^0}{\partial y}, \mathbf{B}_{5,7} = \left(1 + \frac{\partial \Psi_2^k}{\partial z}\right) \frac{\partial \mathbf{N}_{yi}^0}{\partial y} \end{aligned}$$

It should be shown that the coefficients Φ_i^k and Ψ_i^k can be given by

$$\begin{aligned} \Phi_1^k &= f_u^k(z) \\ \Psi_1^k &= f_v^k(z) \\ \Phi_2^k &= \Psi_2^k = z \end{aligned} \tag{23}$$

Once stain matrix can be acquired, the stiffness matrix within one element can be presented by using the following equation.

$$\mathbf{K}^e = \sum_{i=1}^N \int_{z_i}^{z_{i+1}} \left(\iint \mathbf{B}^T \mathbf{Q} \mathbf{B} dx dy \right) dz \tag{24}$$

Utilizing the Hamilton’s principle, equation of motion within one element may be written as

$$\mathbf{M}^e \dot{\mathbf{u}} + \mathbf{K}^e \mathbf{u} = 0 \tag{25}$$

In Eq. (25), the mass matrix \mathbf{M}^e within one element can be presented by

$$\mathbf{M}^e = \int_{A_e} \sum_{i=1}^N \int_{z_i}^{z_{i+1}} \bar{\mathbf{N}}^T \boldsymbol{\rho}_i \bar{\mathbf{N}} dz dA \tag{26}$$

In Eq. (26), the matrices $\bar{\mathbf{N}}$ and $\boldsymbol{\rho}_i$ can be, respectively, expressed as

$$\bar{\mathbf{N}} = [\bar{\mathbf{N}}_1 \bar{\mathbf{N}}_2 \bar{\mathbf{N}}_3] \tag{27}$$

in which

$$\bar{\mathbf{N}}_i = \begin{bmatrix} L_i & 0 & 0 & 0 & 0 & 0 & 0 \\ 0 & L_i & 0 & 0 & 0 & 0 & 0 \\ 0 & 0 & N_i^0 & 0 & N_{xi}^0 & 0 & N_{yi}^0 \\ 0 & 0 & 0 & L_i & 0 & 0 & 0 \\ 0 & 0 & N_{i,x}^0 & 0 & N_{xi,x}^0 & 0 & N_{yi,x}^0 \\ 0 & 0 & 0 & 0 & 0 & L_i & 0 \\ 0 & 0 & N_{i,y}^0 & 0 & N_{xi,y}^0 & 0 & N_{yi,y}^0 \end{bmatrix} \tag{28}$$

$$\boldsymbol{\rho}_i = \rho_i \begin{bmatrix} 1 & 0 & 0 & \Phi_1^k & \Phi_2^k & 0 & 0 \\ 0 & 1 & 0 & 0 & 0 & \Psi_1^k & \Psi_2^k \\ 0 & 0 & 1 & 0 & 0 & 0 & 0 \\ \Phi_1^k & 0 & 0 & \Phi_1^k \Phi_1^k & \Phi_1^k \Phi_2^k & 0 & 0 \\ \Phi_2^k & 0 & 0 & \Phi_2^k \Phi_1^k & \Phi_2^k \Phi_2^k & 0 & 0 \\ 0 & \Psi_1^k & 0 & 0 & 0 & \Psi_1^k \Psi_1^k & \Psi_1^k \Psi_2^k \\ 0 & \Psi_2^k & 0 & 0 & 0 & \Psi_2^k \Psi_1^k & \Psi_2^k \Psi_2^k \end{bmatrix} \tag{29}$$

where ρ_i signifies the density at the i th laminate.

Putting all the element mass and stiffness matrices into the global mass and stiffness matrices according to the order of nodes, the dynamic equation may be presented as

$$\mathbf{M} \ddot{\mathbf{U}} + \mathbf{K} \mathbf{U} = 0 \tag{30}$$

In Eq. (30), \mathbf{M} and \mathbf{K} represent the global mass and stiffness matrices. Natural frequencies of composite and sandwich plates can be acquired by solving the following eigenvalue equation.

$$(\mathbf{K} - \omega^2 \mathbf{M}) \mathbf{U} = 0 \tag{31}$$

where ω denotes frequency of plate.

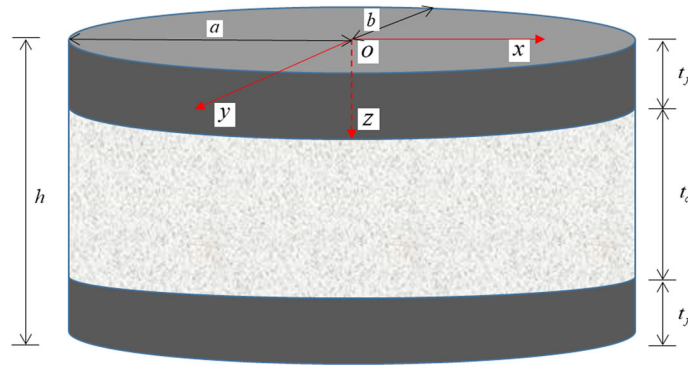


Fig. 1 Geometry and structure of a sandwich ellipse plate

Table 1 Dimensionless frequencies of the clamped circular plate ($h/R = 0.3$)

Models	Modes					
	1	2	3	4	5	6
RFEF (1027 eles)	8.4623	15.5187	22.6347	25.8114	31.0811	35.1154
RFEF (2013 eles)	8.4549	15.4910	22.6173	25.7351	30.9712	34.9811
RFEF (3278 eles)	8.4529	15.4857	22.6096	25.7097	30.9338	34.9555
3D-FEM (43910 eles)	8.4317	15.3950	22.5802	25.0540	29.9645	34.0923
Qin et al. [55]	8.4779	15.5123	22.2614	–	–	–
Civalek and Ersoy [56]	8.4681	15.4594	22.6698	–	–	–
Liew and Yang [57]	8.4676	15.453	22.667	–	–	–

3 Numerical examples

Free vibration of an isotropic plate with clamped boundaries will be firstly investigated, where present results are compared with the published results [55–57]. Subsequently, free vibration analysis of a sandwich circular plate made up of aluminum (Al) sheets and polymethacrylimide (PMI) core is further carried out, which is utilized to account for the performance of the proposed model. In addition, influence of the ratios of major axis to minor axis of ellipse on natural frequencies will be investigated. To improve the stiffness of sandwich plates, we attempt to utilize the composite face sheets to replace the aluminum face sheets. Furthermore, impact of lamination sequence on stiffness of sandwich plate is also investigated.

Example 1 Free vibration analysis of the sandwich circular and ellipse plates with clamped boundaries is carried out to appraise the capability of the proposed model.

In Fig. 1, a , b and h denote length of semimajor axis, length of semiminor axis and height of the sandwich ellipse plate, respectively. In addition, t_c and t_f represent thicknesses of the core layer and face sheets, respectively. As a is equal to b , radius of a circular plate is written as $R = a = b$.

To evaluate performance of the present finite element formulation, free vibration of an isotropic plate with clamped boundaries will be firstly analyzed, in which Young modulus, Poisson ratio and density of material properties are 71 GPa, 0.3 and 2700 kg/m³, respectively. Dimensionless frequencies are defined as $\varpi = \omega R^2 \sqrt{\rho h / D}$, where $D = \frac{Eh^3}{12(1-\nu^2)}$. In Table 1, results obtained from the present model using 1027 elements, 2013 elements and 3278 elements are compared with those presented by Qin et al. [55], Civalek and Ersoy [56], and Liew and Yang [57]. In addition, 3D-FEM results using 43,910 elements are also presented for comparison. Numerical results show that the present results using 2013 elements agree well with the 3D-FEM results, which can verify accuracy of the present model.

Subsequently, free vibration of the sandwich circular and ellipse plates with clamped boundary will be studied. Young modulus, Poisson ratio and density of face sheets made up of the aluminum are 71 GPa, 0.3 and 2700 kg/m³, respectively. For the core layer of PMI, Young modulus, Poisson ratio and density are 92 MPa, 0.375 and 75 kg/m³, respectively. The natural frequencies are normalized as $\varpi = \omega d^2 \sqrt{\rho_s / E_s} / h$, in which $d = 2R$ signifies diameter of circular plate, and $d = 2a$ for an ellipse plate, where a denotes the length of major axis of ellipse; ρ_s and E_s , respectively, denote the density and elastic modulus of face sheets.

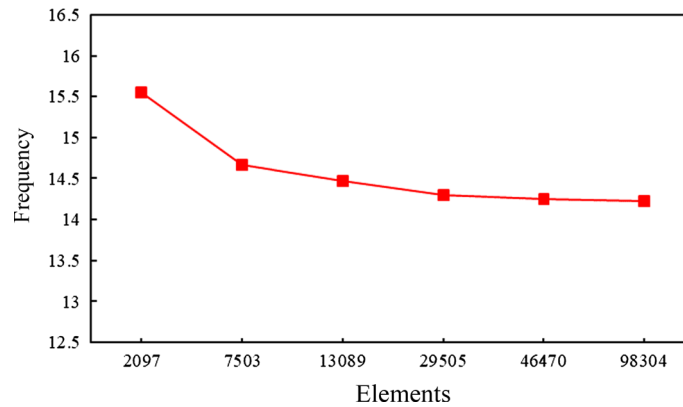


Fig. 2 Variation of natural frequencies acquired from 3D-FEM with increase of elements

Table 2 Comparison of natural frequencies obtained from various models for a three-layer sandwich circular plate ($t_c/t_f = 8$, $d/h = 100$)

Mode number	Models					
	3D-FEM (29,505)	RFEF (2027)	Shi et al. [51] (2018)	Kumar et al. [52] (2019)	Shukla et al. [53] (2019)	Babu et al. [58] (2021)
1	14.2924	14.5202	17.6519	17.7570	17.8852	17.4741
2	25.6723	26.2277	35.5614	35.9571	36.3989	34.9187
3	25.6938	26.2284	35.5468	35.8471	36.4017	34.9275
4	37.3668	38.2933	56.3298	57.0601	58.3167	54.9215
5	37.5971	38.3199	56.3801	57.1056	58.2645	54.9705
6	41.2980	42.2916	63.7517	64.6343	66.1219	62.0311
7	49.6291	50.6626	79.5973	80.8167	83.1365	77.0628
8	49.7664	50.6654	79.5874	80.8051	83.1477	77.0719
9	55.9235	57.2660	93.2885	94.4231	97.9653	90.0261
10	56.1010	57.2713	93.3816	95.3561	98.0051	90.0714
11	62.1737	63.1390	104.842	106.612	110.549	100.846
12	62.2989	63.1455	104.821	106.590	110.526	100.866
13	70.1623	71.7370	124.171	126.367	131.806	118.903
14	70.7425	71.8049	124.342	126.455	131.994	119.066
15	72.8193	74.2659	130.124	132.797	138.396	124.428
16	74.8638	75.6493	131.695	134.013	140.107	125.948
17	75.1452	75.6415	131.707	134.027	140.094	125.958
18	84.6749	85.9656	156.248	159.059	167.573	148.626
19	84.7601	85.9797	156.293	159.027	167.532	148.664
20	87.7623	88.1371	159.898	162.699	171.511	152.053

It requires to be indicated that three-dimensional elasticity solutions of natural frequencies for the sandwich circular and ellipse plates are less reported in the published literature. Thus, the results acquired from 3D-FEM will be selected for a reference to appraise the present model as well as the chosen models. Firstly, variation of 3D-FEM results with refinement of meshes is depicted in Fig. 2, which shows that the converged results can be obtained by using the 3D-FEM with 29,505 elements.

In order to explore the capability of the proposed model predicting the higher-order frequencies, the first twenty frequencies of sandwich circular plate are compared with the 3D-FEM results in Table 2, where four kinds of Reddy-type higher-order models recently proposed by Shi et al. [51], Kumar et al. [52], Shukla et al. [53] and Babu et al. [58] are also selected for comparison. Differing from the present model, the shear deformation functions of the selected models can be written as $f(z) = (h/2)\tanh(2z/h) - z/\cosh^2(1)$ [51], $f(z) = \sin(2p\pi z/h) - (2p\pi z/h)\cos(p\pi)$ where $p = 0.6$ [52], $f(z) = \sin(2p\pi z/h) - (2p\pi z/h)\cos(p\pi)$ where $p = 0.4$ [53], and $f(z) = g(z) + z\Omega$ where $g(z) = \sinh^{-1}(rz/h)$, $\Omega = -2r/(h\sqrt{r^2 + 4})$ and $r = 3$ [58]. Typical finite element mesh configuration with 2027 elements has been depicted in Fig. 3. In Fig. 4, displacement modes corresponding to the higher-order frequencies are depicted, which can help to understand well the vibration modes of sandwich circular plate.

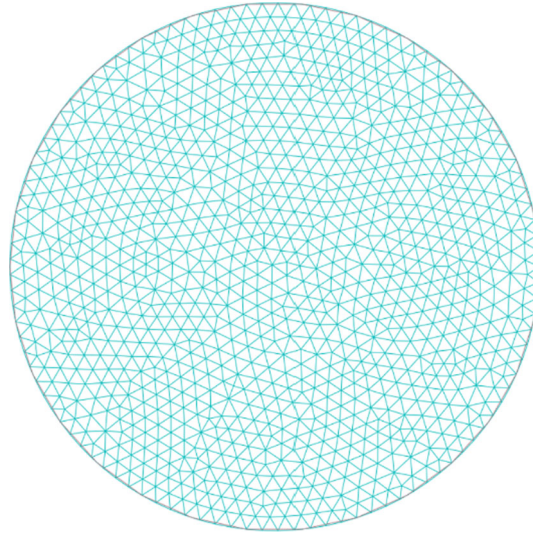


Fig. 3 Typical finite element mesh configuration with 2027 elements

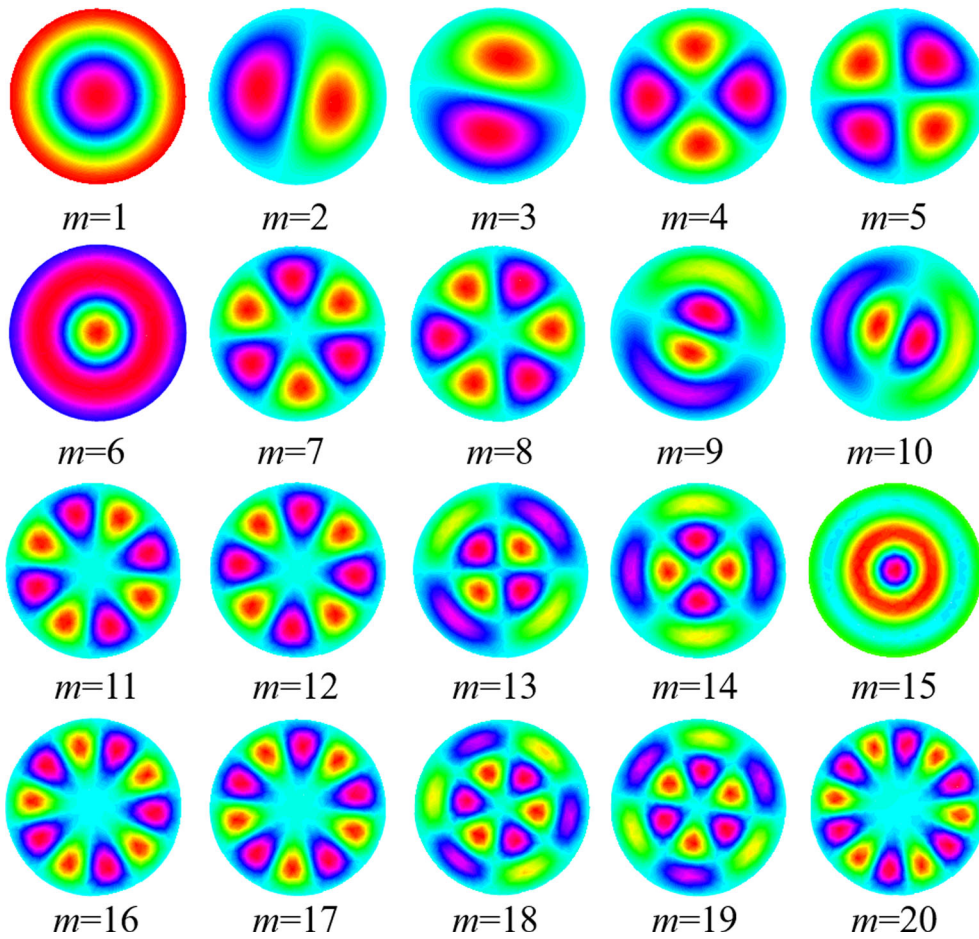
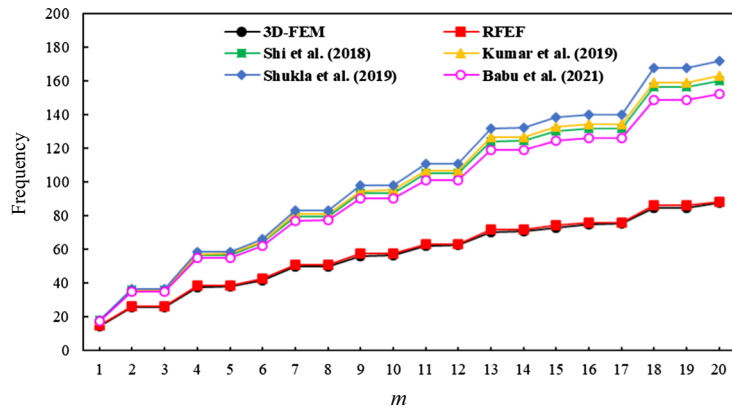
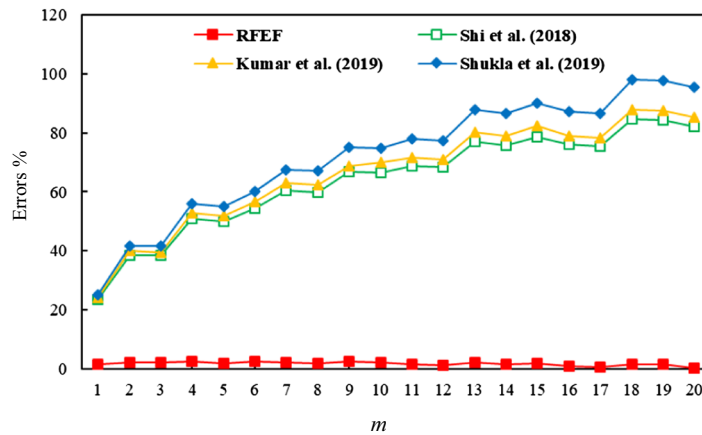


Fig. 4 Displacement modes of a three-ply sandwich circular plate with clamped boundaries ($t_c/t_f = 8$, $d/h = 100$)



(a) Comparison between results acquired from various models and 3D-FEM results



(b) Percentage errors of results acquired from various models relative to 3D-FEM results

Fig. 5 Comparison of natural frequencies acquired from various models for a three-layer sandwich circular plate ($t_c/t_f = 8$, $d/h = 100$)

In addition, all results in Table 2 are plotted in Fig. 5a. It can be noted that curved line of the results acquired from present model RFEF nearly covers that of 3D-FEM results. With increase of mode number, complex deformation of sandwich plate will occur, so that the zig-zag effect plays the more important rule in structural deformation. Thus, natural frequencies acquired from the selected models discarding the zig-zag effect [51–53, 58] rapidly deviate the 3D-FEM results. Furthermore, it can be observed that when mode number is more than 17, divergence between these results and 3D-FEM results is rapidly aggravated. For the sake of accounting for such appearance, the percentage errors of results acquired from the selected models relative to 3D-FEM results are depicted in Fig. 5b. Numerical results indicate that the maximum error of the present model is less than 2.5%. However, the maximum errors of other models are more than 80%.

To extend range of application of the proposed model, natural frequencies of the sandwich ellipse plate with major axis a along x direction and minor axis b along y direction are analyzed, which are shown in Table 3. The first twenty displacement modes corresponding to diverse frequencies are depicted in Fig. 6. Variation of displacement modes in the ellipse plate evidently differs from those of the circular plate attributing to dissimilar stiffness along x and y directions. In fact, bending stiffness along the long axis is smaller than that of short axis, so that bending deformation along the long axis more easily occurs in comparison with deformation along the short axis. All results in Table 3 are plotted in Fig. 7 in conjunction with 3D-FEM results. Again, curved line of the results acquired from the present model RFEF covers exactly the curved line of 3D-FEM results, which may illustrate well the capability of the proposed model for a sandwich ellipse plate.

In addition, impact of the ratios of major axis a to minor axis b on natural frequencies is to be researched. Natural frequencies of sandwich ellipse plates with diverse ratios of a/b are shown in Table 4. In order to

Table 3 Comparison of natural frequencies obtained from various models for a three-layer sandwich ellipse plate ($t_c/t_f = 8$, $a/h = 50$, $a/b = 0.5$)

Mode number	Models					
	3D-FEM (58,245)	RFEF (4398)	Shi et al. [51]	Kumar et al. [52]	Shukla et al. [53]	Babu et al. [58]
1	10.0568	10.1662	11.9191	11.9840	12.0451	11.8238
2	13.9231	14.0851	17.0501	17.1513	17.2765	16.8782
3	18.8319	19.0772	23.9273	24.0771	24.3194	23.6287
4	21.8957	22.2942	29.4467	29.7778	30.0791	28.9824
5	24.5617	24.9198	32.5249	32.7353	33.1784	32.0269
6	26.5032	26.9795	36.6941	37.1278	37.6091	36.0241
7	30.9375	31.3999	42.7618	43.0423	43.8048	41.9678
8	31.7636	32.2649	45.2520	45.8038	46.5485	44.3045
9	35.9588	36.7518	53.6874	54.6397	55.5077	52.3945
10	37.5126	38.0691	54.5177	54.8716	56.1099	53.3105
11	37.7944	38.3452	55.0985	55.7788	56.8972	53.7877
12	41.1666	41.9459	62.8511	63.9884	65.2216	61.1741
13	43.7192	44.2854	66.1982	67.0101	68.6430	64.4221
14	45.0106	45.6114	67.6483	68.0688	69.9769	65.8931
15	46.8166	47.5116	73.1094	74.4405	76.1583	70.9600
16	50.2962	50.8452	78.4912	79.4278	81.7467	76.1353
17	51.3312	52.3483	82.0097	82.4768	85.2847	79.5590
18	52.4264	53.0989	83.3333	85.3873	87.2800	80.6253
19	52.7777	53.4274	84.4185	85.9396	88.2874	81.7003
20	56.8752	57.6569	94.0644	96.3826	98.8870	88.8177

Table 4 Effect of the chosen parameters on the first natural frequencies of the three-layer sandwich plates ($a/h = 50$, $t_c/t_f = 8$)

a/b	3D-FEM	RFEF	Shukla et al. [53]
0.50	10.0568	10.1662	12.0451
0.75	11.7845	11.9311	14.2715
1.00	14.2924	14.5596	17.8733
1.25	17.3684	17.7586	22.9792
1.50	20.7819	21.4513	29.42682
1.75	24.5362	25.3942	37.0464
2.00	28.3594	29.6547	45.7181
2.50	36.1444	38.0572	65.5428
3.00	43.9487	46.7739	88.1532

explicitly illustrate performance of different models, results in Table 4 are depicted in Fig. 8. In Fig. 8a, results acquired from the present model RFEF are consistent well with the 3D-FEM results, but a slight divergence from 3D-FEM can be noted with increase of the ratios of major axis a and minor axis b . Furthermore, the maximum error of present model RFEF reaches at 6.43% for $a/b = 3$, which can be found in Fig. 8b.

Example 2 Free vibration of the clamped sandwich circular plate with composite face sheets and PMI core is analyzed.

In this case, material properties of face sheets [59] are $E_1 = 181$ GPa, $E_2 = 10.3$ GPa, $E_3 = E_2$, $G_{12} = 7.17$ GPa, $G_{13} = G_{12}$, $G_{23} = 2.87$ GPa, $\nu_{12} = 0.25$, $\nu_{13} = 0.25$ and $\nu_{23} = 0.33$, where subscripts '1' and '2' denote the direction parallel to the fibers and the direction vertical to the fibers in the 1–2 plane, respectively; subscript '3' denotes the direction vertical to the 1–2 plane. Material properties of PMI core can be found in example 1. The natural frequencies are normalized as $\bar{\omega} = \omega d^2 \sqrt{\rho_s / E_{2s}} / h$, where the density of face sheet $\rho_s = 1578$ kg/m³, and elastic modulus $E_{2s} = 10.3$ GPa.

Firstly, performance of the proposed model predicting natural frequencies of the sandwich circular plate with composite face sheets and PMI core will be researched, which is the foundations studying an impact of face sheets on frequencies. In Table 5, results acquired from the higher-order models are compared with the 3D-FEM results. It can be noted that present results are in good agreement with the 3D-FEM results. Nevertheless, the results obtained from the selected higher-order models [51–53, 58] are largely more than the 3D-FEM results, as these models are unable to fulfill continuity conditions of interlaminar stresses. In order to illustrate the relationships between the results obtained from the five-unknown higher-order models and

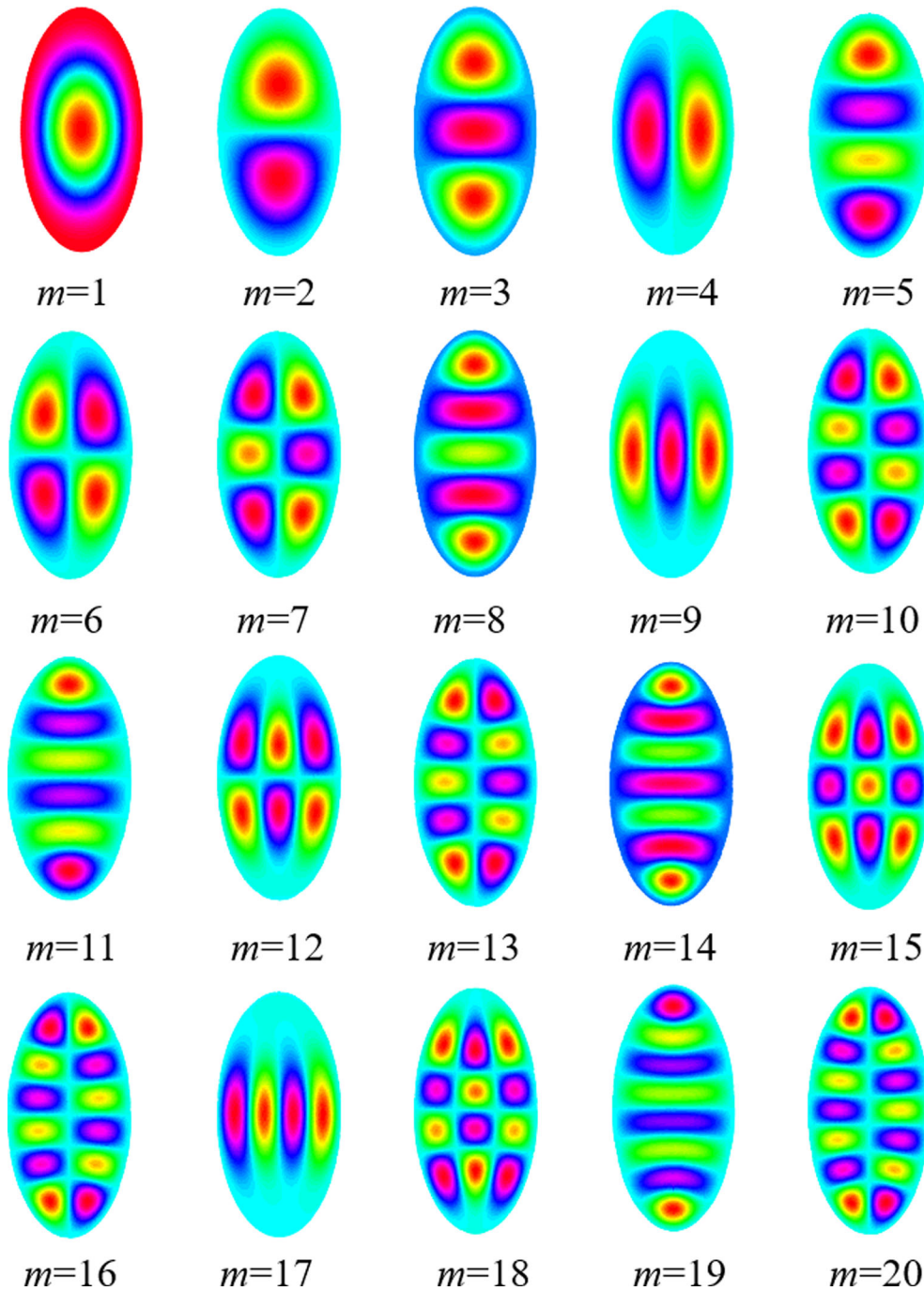


Fig. 6 Displacement modes of a three-ply sandwich ellipse plate with clamped boundaries ($t_c/t_f = 8$, $alh = 50$, $alb = 0.5$)

the 3D-FEM results, all results in Table 5 have been plotted in Fig. 9, and it is found that several frequencies acquired from the present model corresponding to displacement modes 13, 16 and 20 are slight diverse from the 3D-FEM results. However, present results corresponding to other displacement modes are in exact agreement with the 3D-FEM results.

In addition, natural frequencies of the same size sandwich plate made up of composite face sheets and PMI core are compared with those of the sandwich plate composed of aluminum face sheets and PMI core in Fig. 10. Numerical comparison reveals that the natural frequencies of sandwich circular plate made up of composite

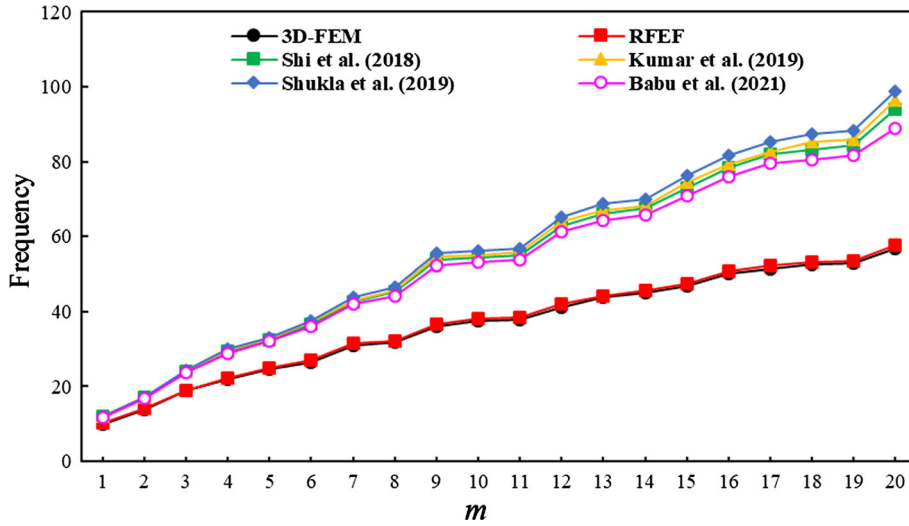
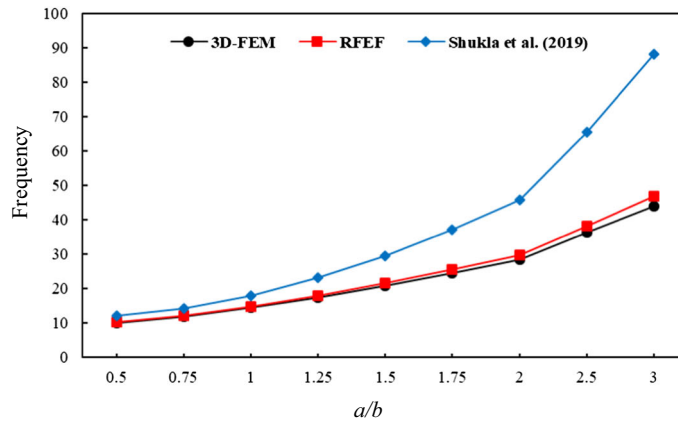
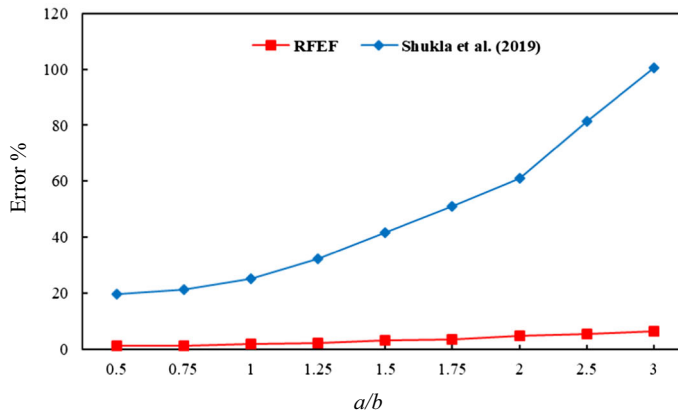


Fig. 7 Comparison of natural frequencies obtained from various models for a three-layer sandwich ellipse plate ($t_c/t_f = 8$, $alh = 50$, $a/b = 0.5$)



(a) Comparison between results acquired from various models and 3D-FEM results



(b) Percentage errors of results acquired from various models relative to 3D-FEM results

Fig. 8 Effect of the chosen parameters on the first natural frequencies of the three-layer sandwich plates ($alh = 50$, $t_c/t_f = 8$)

Table 5 Comparison of natural frequencies obtained from various models for a three-layer sandwich circle plate with composite face sheets ($t_c/t_f = 8, d/h = 100$)

Mode number	m, n						
		3D-FEM (29,676)	RFEF (4288)	Shi et al. [51]	Kumar et al. [52]	Shukla et al. [53]	Babu et al. [58]
1		31.6270	32.3295	38.6527	39.3677	40.1810	37.8190
2		44.7085	45.3281	52.7879	53.4721	54.7035	51.7542
3		64.3049	64.8192	73.7384	74.1726	76.1420	72.4513
4		64.3561	66.6088	87.0729	89.8408	93.0365	84.0211
5		78.7625	80.9964	103.649	106.270	110.439	99.2372
6		89.0935	89.5467	100.919	100.746	104.044	100.180
7		98.3568	100.430	125.548	127.742	133.271	121.605
8		101.946	106.268	133.329	132.057	137.546	131.015
9		117.536	117.964	146.105	152.059	159.202	139.726
10		118.259	122.400	152.412	153.706	161.212	147.895
11		122.174	124.130	164.801	166.697	175.439	157.939
12		139.477	143.239	170.215	170.668	179.508	166.899
13		141.283	147.617	183.659	183.452	193.784	178.385
14		147.355	148.416	188.605	192.907	203.886	181.053
15		149.030	151.068	209.868	204.487	217.767	200.015
16		158.992	165.189	210.550	216.246	230.462	205.331
17		165.433	168.732	218.602	219.446	232.868	208.551
18		177.314	179.216	216.783	220.531	233.335	212.241
19		177.491	179.890	231.457	240.096	254.955	220.307
20		181.097	186.827	249.184	243.155	266.977	240.219

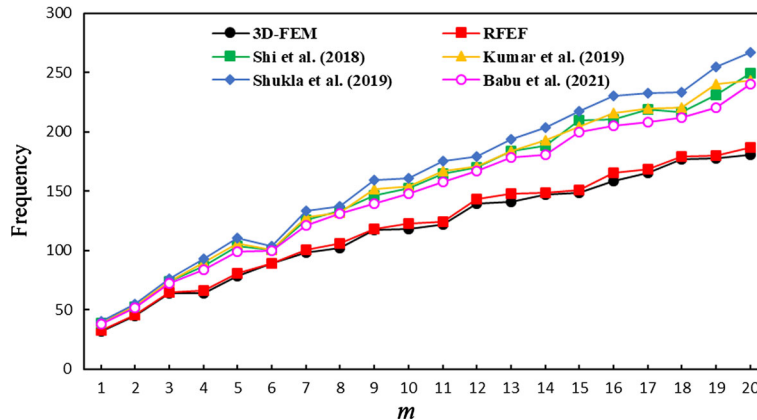


Fig. 9 Comparison of natural frequencies obtained from various models for a three-layer sandwich circle plate with composite face sheets ($t_c/t_f = 8, d/h = 100$)

face sheets have been significantly improved, which imply that relative stiffness of sandwich circular plate can be largely elevated by utilizing the composite face sheets to replace aluminum face sheets.

In the above study, it can be observed that if aluminum face sheets are replaced by composite face sheets, the stiffness of sandwich circular plate can be significantly elevated, so an approach increasing the stiffness of sandwich circular plate should be explored. Therefore, configuration of face sheets will be designed to improve stiffness of such structure. As a result, three groups of sandwich plates containing aluminum face sheets [Al/C/Al] (Sandwich-1), composite face sheets [0°/C/0°] (Sandwich-2) and composite face sheets [0°/90°/C/90°/0°] (Sandwich-3) will be analyzed, and all results have been shown in Table 6 in conjunction with 3D-FEM results.

To find out variation of natural frequencies, all results in Table 6 have been plotted in Fig. 11. Numerical results imply that relative stiffness of sandwich circular plate can be surely elevated by using the composite face sheets. In addition, the relative stiffness of sandwich circular plate can be further elevated by changing the laminated configuration. For example, stiffness of sandwich plate [0°/90°/C/90°/0°] is explicitly more than that of sandwich plate [0°/C/0°], which can show that composite face sheets possess the designability.

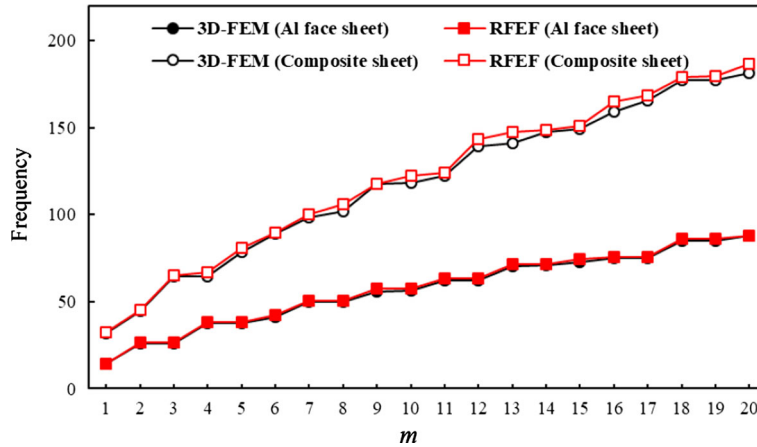


Fig. 10 Comparison of natural frequencies for the three-layer sandwich circle plates with aluminum face sheet and composite face sheets ($t_c/t_f = 8, d/h = 100$)

Table 6 Comparison of natural frequencies obtained from various models for the sandwich circle plates with different face sheets ($t_c/t_f = 18, d/h = 100$)

Mode number	[Al/C/Al]		[0°/C/0°]		[0°/90°/C/90°/0°]	
	3D-FEM (70,221)	RFEF (2027)	3D-FEM (87,345)	RFEF (2027)	3D-FEM (68,825)	RFEF (2027)
1	15.6265	15.8338	34.7300	35.1679	38.3301	39.0444
2	29.1842	29.8176	48.8278	48.6155	70.5575	72.9242
3	29.2024	29.8221	70.0104	68.9846	72.4061	74.7488
4	43.5039	44.6956	74.5454	76.4452	103.847	107.542
5	43.5270	44.7311	90.5898	91.8590	109.314	114.755
6	48.3412	49.7778	98.1845	95.5105	118.474	123.812
7	58.4423	60.2703	112.540	112.765	142.642	149.197
8	58.4810	60.2744	121.699	125.297	144.367	150.546
9	66.6260	68.9046	130.997	127.378	162.382	170.061
10	66.7401	68.8818	139.986	138.665	166.853	175.253
11	73.7275	76.2473	140.314	143.007	182.055	190.759
12	73.9052	76.2581	164.668	162.696	182.886	191.225
13	84.6749	87.6142	168.507	165.740	205.977	214.009
14	84.7108	87.7122	171.620	168.935	211.120	222.693
15	87.8922	91.0018	172.488	177.937	220.241	231.365
16	89.3810	92.4675	193.391	193.444	221.679	232.705
17	89.4788	92.4596	195.094	196.972	223.407	232.830
18	102.469	106.182	206.271	200.258	252.632	263.129
19	102.745	106.204	207.884	202.980	255.559	266.433
20	104.964	112.017	219.358	221.096	262.932	275.026

4 Conclusions

IN this work, a finite element formulation is developed for free vibration analysis of sandwich circular and ellipse plates. Compared to the existing five-variable theories, the present model can fulfill in advance compatible conditions of transverse shear stresses at the adjacent laminates, but they possess the same displacement parameters. Strain components of present model have the second derivatives, so the refined-element method is utilized to overcome the compatible requirement of the first derivatives of transverse displacement at the shared edge of the adjacent elements. In order to appraise capability of the proposed model, free vibration analysis of sandwich circular plate with aluminum face sheets and PMI core is firstly carried out. Subsequently, effect of ratios of major axis to minor axis for an ellipse plate on natural frequencies is further studied. An approach improving the stiffness of sandwich plates is also discussed by changing the face sheets. By means of the outcome of analysis, the following conclusions will be drawn:

- (1) Possessing the same expression of displacements, the proposed model can more precisely produce natural frequencies of sandwich circular and ellipse plates than the existing five-variable higher-order models.

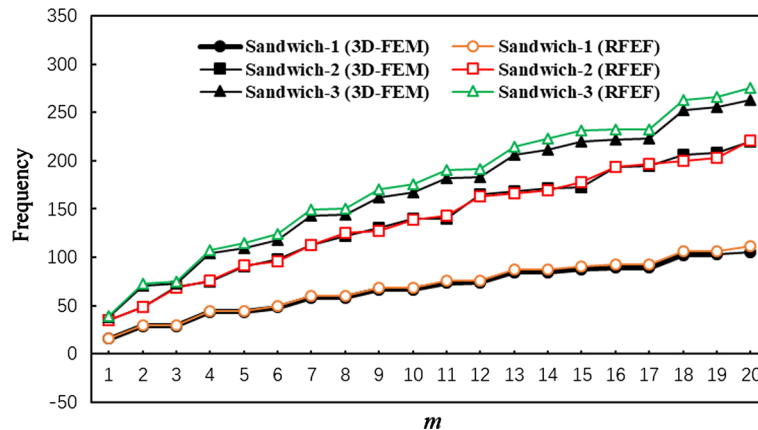


Fig. 11 Comparison of natural frequencies obtained from various models for the sandwich circle plates with different face sheets ($t_c/t_f = 18$, $d/h = 100$)

- (2) Variation of displacement modes in the ellipse plate evidently differs from those of the circular plate attributing to dissimilar stiffness along x and y directions. Moreover, the ratios of major axis a to minor axis b influence the capability of the models predicting natural frequencies.
- (3) The relative stiffness of sandwich circular plate can be surely elevated by using the composite face sheets. Moreover, the relative stiffness of sandwich circular plate can be further elevated by changing the lamination configuration, which can account for the designability of sandwich plate with composite face sheets.

Acknowledgements The work described in this paper was supported by the National Natural Science Foundation of China [No. 12172295].

Declarations

Conflict of interest The author(s) declared no potential conflicts of interest with respect to the research, authorship, and/or publication of this article.

References

1. Weisensel, G.N.: Natural frequency information for circular and annular plates. *J. Sound Vib.* **133**(1), 129–137 (1989)
2. Reissner, E.: The effect of transverse shear deformation on the bending of elastic plates. *J. Appl. Mech.* **12**(2), 69–72 (1945)
3. Mindlin, R.D.: Influence of rotary inertia and shear on flexural motions of isotropic Elastic Plates. *J. Appl. Mech.* **18**(1), 31–38 (1951)
4. Pagano, N.J.: Exact solutions for rectangular bi-directional composites. *J. Compos. Mater.* **4**, 20–34 (1970)
5. Reddy, J.N., Chen, Z.Q.: Three-dimensional thermomechanical deformations of functionally graded rectangular plates. *Eur. J. Mech. A/Solids* **20**, 841–855 (2001)
6. Whitney, J.M., Sun, C.T.: A higher order theory for extensional motion of laminated composites. *J. Sound Vib.* **30**(1), 85–97 (1973)
7. Reddy, J.N.: A simple higher-order theory for laminated composite plates. *J. Appl. Mech.* **51**, 745–752 (1984)
8. Kant, T., Swaminathan, K.: Analytical solution for free vibration of laminated composite and sandwich plates based on a higher-order refined theory. *Compos. Struct.* **53**, 73–85 (2001)
9. Sofiyev, A.H.: The vibration and buckling of sandwich cylindrical shells covered by different coatings subjected to the hydrostatic pressure. *Compos. Struct.* **117**, 124–134 (2014)
10. Meiche, N.E., Tounsi, A., Ziane, N., Mechab, I., Bedia, E.A.A.: A new hyperbolic shear deformation theory for buckling and vibration of functionally graded sandwich plate. *Int. J. Mech. Sci.* **53**(4), 237–247 (2011)
11. Matsunaga, H.: Vibration and stability of cross-ply laminated composite plates according to a global higher-order plate theory. *Compos. Struct.* **48**, 231–244 (2000)
12. Matsunaga, H.: Vibration and buckling of multilayered composite beam according to higher order deformation theories. *J. Sound Vib.* **246**, 47–62 (2001)
13. Matsunaga, H.: Vibration and stability of angle-ply laminated composite plates subjected to in-plane stresses. *Int. J. Mech. Sci.* **43**, 1925–1944 (2001)
14. Nayak, A.K., Moy, S.S.J., Shenoi, R.A.: Free vibration analysis of composite sandwich plates based on Reddy's higher-order theory. *Compos. B Eng.* **33**, 505–519 (2002)

15. Jin, G.Y., Yang, C.M., Liu, Z.G.: Vibration and damping analysis of sandwich viscoelastic-core using Reddy's higher-order theory beam. *Compos. Struct.* **140**, 390–409 (2016)
16. Tomar, S.S., Talha, M.: Influence of material uncertainties on vibration and bending behaviour of skewed sandwich FGM plates. *Compos. B Eng.* **163**, 779–793 (2019)
17. Bennoun, M., Houari, M.S.A., Tounsi, A.: A novel five-variable refined plate theory for vibration analysis of functionally graded sandwich plates. *Mech. Adv. Mater. Struct.* **23**(4), 423–431 (2016)
18. Rao, M.K., Desai, Y.M.: Analytical solutions for vibrations of laminated and sandwich plates using mixed theory. *Compos. Struct.* **63**, 361–373 (2004)
19. Rao, M.K., Scherbatiuk, K., Desai, Y.M., Shah, A.H.: Natural vibrations of laminated and sandwich plates. *J. Eng. Mech.* **130**(11), 1268–1278 (2004)
20. Belarbi, M., Tati, A., Ounis, H., Khechai, A.: On the free vibration analysis of laminated composite and sandwich plates: a layerwise finite element formulation. *Latin Am. J Solids Struct.* **14**(12), 2265–2290 (2017)
21. Murakimi, H.: Laminated composite plate theory with improved in-plane responses. *J. Appl. Mech.* **53**, 661–666 (1986)
22. Zhen, Wu.: Chen WJ, An assessment of several displacement-based theories for the vibration and stability analysis of laminated composite and sandwich beams. *Compos. Struct.* **84**(4), 337–349 (2008)
23. Orakdögen, E., Küçükarslan, S., Sofiyev, A., Omurtag, M.H.: Finite element analysis of functionally graded plates for coupling effect of extension and bending. *Meccanica* **45**, 63–72 (2010)
24. Sofiyev, A.H., Osmancebioglu, E.: The free vibration of sandwich truncated conical shells containing functionally graded layers within the shear deformation theory. *Compos. B* **120**, 197–211 (2017)
25. Sofiyev, A.H.: Application of the FOSDT to the solution of buckling problem of FGM sandwich conical shells under hydrostatic pressure. *Compos. B* **144**, 88–98 (2018)
26. Hacıyev, V.C., Sofiyev, A.H., Kuruoglu, N.: Free bending vibration analysis of thin bidirectionally exponentially graded orthotropic rectangular plates resting on two-parameter elastic foundations. *Compos. Struct.* **184**, 372–377 (2018)
27. Sofiyev, A.H.: Review of research on the vibration and buckling of the FGM conical shells. *Compos. Struct.* **211**, 301–317 (2019)
28. Sofiyev, A.H., Fantuzzi, N.: Analytical solution of stability and vibration problem of clamped cylindrical shells containing functionally graded layers within shear deformation theory. *Alex. Eng. J.* (2022). <https://doi.org/10.1016/j.aej.2022.08.024>
29. Avcar, M., Hadji, L., Civalek, O.: Natural frequency analysis of sigmoid functionally graded sandwich beams in the framework of high order shear deformation theory. *Compos. Struct.* **276**, 114564 (2021)
30. Hadji, L., Avcar, M.: Free vibration analysis of FG porous sandwich plates under various boundary conditions. *J. Appl. Comput. Mech.* **7**(2), 505–519 (2021)
31. Belarbi, M.O., Zenkour, A.M., Tati, A., Salami, S.J., Khechai, A., Houari, M.S.A.: An efficient eight-node quadrilateral element for free vibration analysis of multilayer sandwich plates. *Int. J. Numer. Methods Eng.* **122**, 2360–2387 (2021)
32. Hadji, L., Avcar, M., Zouatnia, N.: Natural frequency analysis of imperfect FG sandwich plates resting on Winkler-Pasternak foundation. *Mater. Today: Proc.* **53**, 153–160 (2022)
33. Hirane, H., Belarbi, M.O., Houari, M.S.A., Tounsi, A.: On the layerwise finite element formulation for static and free vibration analysis of functionally graded sandwich plates. *Eng. Comput.* (2021). <https://doi.org/10.1007/s00366-020-01250-1>
34. Garg, A., Chalak, H.D., Li, L., Belarbi, M.O., Sahoo, R., Mukhopadhyay, T.: Vibration and buckling analyses of sandwich plates containing functionally graded metal foam core. *Acta Mech. Solida Sin.* **35**(4), 587–602 (2022)
35. Vinh, P.V., Huy, L.Q.: Finite element analysis of functionally graded sandwich plates with porosity via a new hyperbolic shear deformation theory. *Def. Technol.* **18**, 490–508 (2022)
36. Vinh, P.V., Chinh, N.V., Tounsi, A.: Static bending and buckling analysis of bi-directional functionally graded porous plates using an improved first-order shear deformation theory and FEM. *Eur. J. Mech. A Solids* **96**, 104743 (2022)
37. Birman, V., Kardomateas, G.A.: Review of current trends in research and applications of sandwich structures. *Compos. B Eng.* **142**, 221–240 (2018)
38. Ebrahimi, F., Rastgo, A.: An analytical study on the free vibration of smart circular thin FGM plate based on classical plate theory. *Thin-Walled Struct.* **46**(12), 1402–1408 (2008)
39. Liu, X., Wang, Q., Quek, S.T.: Analytical solution for free vibration of piezoelectric coupled moderately thick circular plates. *Int. J. Solids Struct.* **39**(8), 2129–2151 (2002)
40. Qiu, X., Deshpande, V.S., Fleck, N.A.: Dynamic response of a clamped circular sandwich plate subject to shock loading. *J. Appl. Mech.* **71**(5), 637–645 (2004)
41. Du, G.J., Ma, J.Q.: Nonlinear vibration and buckling of circular sandwich plate under complex load. *Appl. Math. Mech.* **28**(8), 1081–1091 (2007)
42. Hashemi, S.H., Eshaghi, M., Karimi, M.: Closed-form vibration analysis of thick annular functionally graded plates with integrated piezoelectric layers. *Int. J. Mech. Sci.* **52**(3), 410–428 (2010)
43. Sharma, P., Parashar, S.K.: Free vibration analysis of shear-induced flexural vibration of FGPM annular plate using generalized differential quadrature method. *Compos. Struct.* **155**, 213–222 (2016)
44. Jandaghian, A.A., Jafari, A.A., Rahmani, O.: Vibrational response of functionally graded circular plate integrated with piezoelectric layers: an exact solution. *Eng. Solid Mech.* **2**(2), 119–130 (2014)
45. Oveisi, A., Shakeri, R.: Robust reliable control in vibration suppression of sandwich circular plates. *Eng. Struct.* **116**, 1–11 (2016)
46. Mao, R., Lu, G., Wang, Z.: Large deflection behavior of circular sandwich plates with metal foam-core. *Eur. J. Mech A-solids* **55**, 57–66 (2016)
47. Starovoitov, E.I., Leonenko, D.V.: Vibrations of circular composite plates on an elastic foundation under the action of local loads. *Mech. Compos. Mater.* **52**(5), 665–672 (2016)
48. Shishehsaz, M., Raissi, H., Moradi, S.: Stress distribution in a five-layer circular sandwich composite plate based on the third and hyperbolic shear deformation theories. *Mech. Adv. Mater. Struct.* **27**(11), 927–940 (2020)
49. Shahrokhi, M., Jomehzadeh, E., Rezaeizadeh, M.: Piezoelectricity and length scale effect on the vibrational behaviors of circular sandwich micro-plates. *J. Sandwich Struct. Mater.* **23**(1), 279–300 (2021)

50. Cheung, Y.K., Chen, W.J.: Refined nine-parameter triangular thin plate bending element by using refined direct stiffness method. *Int. J. Numer. Methods Eng.* **38**, 283–298 (1995)
51. Shi, P., Dong, C.Y., Sun, F., Liu, W., Hu, Q.: A new higher order shear deformation theory for static, vibration and buckling responses of laminated plates with the isogeometric analysis. *Compos. Struct.* **204**, 342–358 (2018)
52. Kumar, R., Lal, A., Singh, B.N., Singh, J.: New transverse shear deformation theory for bending analysis of FGM plate under patch load. *Compos. Struct.* **208**, 91–100 (2019)
53. Shukla, A., Vishwakarma, P.C., Singh, J., Singh, J.: Vibration analysis of angle-ply Laminated Plates with RBF based Meshless approach. *Mater. Today Proc.* **18**, 4605–4612 (2019)
54. Bazeley, G.P., Cheung, Y.K., Irons, B.M., Zienkiewicz, O.C.: Triangular elements in bending conforming and non-conforming solution. *Proc. Conf. Matrix Methods Struct. Mech.* **7**, 547–576 (1965)
55. Qin, X., Shen, Y., Chen, W., Yang, J., Peng, L.X.: Bending and free vibration analyses of circular stiffened plates using the FSDT mesh-free method. *Int. J. Mech. Sci.* **202–203**, 106498 (2021)
56. Civalek, O., Ersoy, H.: Free vibration and bending analysis of circular Mindlin plates using singular convolution method. *Commun. Numer. Meth. Eng.* **25**, 907–922 (2009)
57. Liew, K.M., Yang, B.: Three-dimensional elasticity solutions for free vibration of circular plates: a polynomials-Ritz analysis. *Comput. Methods Appl. Mech. Eng.* **175**, 189–201 (1999)
58. Babu, R.T., Verma, S.V., Singh, B.N., Maiti, D.K.: Dynamic analysis of flat and folded laminated composite plates under hygrothermal environment using a nonpolynomial shear deformation theory. *Compos. Struct.* **274**, 114327 (2021)
59. Kapuria, S., Dumir, P.C., Jain, N.K.: Assessment of zigzag theory for static loading, buckling, free and forced response of composite and sandwich beams. *Compos. Struct.* **64**, 317–327 (2004)

Publisher's Note Springer Nature remains neutral with regard to jurisdictional claims in published maps and institutional affiliations.

Springer Nature or its licensor (e.g. a society or other partner) holds exclusive rights to this article under a publishing agreement with the author(s) or other rightsholder(s); author self-archiving of the accepted manuscript version of this article is solely governed by the terms of such publishing agreement and applicable law.